Chapter 16

Uncovering Metabolic Effects of Anti-angiogenic Therapy in Tumors by Induced Metabolic Bioluminescence Imaging

Stefano Indraccolo, Stefan Walenta, and Wolfgang Mueller-Klieser

Abstract

Induced metabolic bioluminescence imaging (imBI) is an imaging technique which enables detection of various metabolites associated with glycolysis in tumor sections. Signals captured by imBI can be used to chart the topographic distribution of lactate, glucose, pyruvate, and ATP and quantify their absolute amount. ImBi can enable us to perform metabolic classification of tumors as well as to detect metabolic changes in the glycolytic pathway associated with certain therapies, such as anti-angiogenic drugs.

Key words Tumor xenografts, Bioluminescence, Glycolysis, Angiogenesis, Imaging

1 Introduction

Angiogenesis plays an essential role in tumor growth and metastasis and tumor angiogenesis pathways have been identified as important therapeutic targets in many types of cancer. Vascular endothelial growth factor (VEGF) is one of the key cytokines driving tumor angiogenesis. By targeting the tumor-associated microvasculature, VEGF signaling inhibitors cause vessel pruning, which is followed by hypoxia and reduced supply of other nutrients [1–4]. Since anti-angiogenic drugs do not have, in general, direct effects of tumor cells, the therapeutic activity of these drugs is almost entirely dependent on its modulation of the supportive functions of the tumor microenvironment. Albeit still hypothetical, it is quite possible that the metabolic status of tumor cells can enable them to either succumb or adapt to the starving effects on anti-angiogenic therapy. Tumor metabolism could eventually represent a factor that influences tumor response to VEGF inhibitors.

Imaging techniques are extremely valuable both to perform metabolic profiling of tumors and to uncover metabolic fluctuations caused by drugs. With regard to anti-angiogenic therapy, some of these techniques have been used to measure the uptake of selected metabolites in tumors, such as PET [5], whereas others,

Domenico Ribatti (ed.), *Tumor Angiogenesis Assays: Methods and Protocols,* Methods in Molecular Biology, vol. 1464,
DOI 10.1007/978-1-4939-3999-2_16,

including hyperpolarized ^{13}C spectroscopy [6] and proton NMR [7], enabled quantitative assessment of certain metabolites in experimental tumors.

We were the first to exploit a technique termed induced metabolic bioluminescence imaging (imBI) to investigate metabolic perturbations associated with anti-VEGF therapy [5, 8]. Notably, although somewhat limited by the small number of metabolites which can be analyzed, imBI provides an accurate representation of the steady-state levels of the metabolites, matching them to the histology of the tumor section.

The imBI technique has been developed in the laboratory at the University of Mainz to detect metabolites in cryo-sections from snap-frozen tissue in situ [9–11] (*see* **Note 1**). The data obtained therefore reflect a "snapshot" of the momentary metabolic status of biological tissues. Self-made kits containing definite exogenous enzymes and cofactors are used as "metabolic sensors" to achieve high specificity and sensitivity. Heat inactivation of endogenous enzyme activities in the tissue sections of interest immediately before imBI measurement avoids interference with exogenous enzymes within the kit. Substrate saturation is prevented by providing all components of the kit in excess. The enzymatic activity induced by the metabolite of interest in the target tissue is biochemically coupled via the $NAD(P)H+H^+$ redox system to luciferases leading to light emission, i.e., to bioluminescence. The intensity of this low-level light emission is proportional to the tissue content of the respective metabolite. The biochemistry for the detection of ATP, glucose, pyruvate, and lactate via imBI is illustrated diagrammatically in Fig. 1. Since a specific enzyme mixture has to be prepared for each metabolite of interest, the imBI technique allows for the detection of only one metabolite per section. On the other hand, section thickness is adjusted in most cases to values in the range of 10–20 μm, and thus different metabolites can be determined in serial sections at a quasi-identical location within a tissue. Furthermore, a specific computerized overlay technique using metabolic and structural imaging allows for the determination of metabolite concentrations within selected histological tissue areas.

The rest of this chapter is devoted to the methodologic description of this valuable imaging technique and its applications in the field of tumor angiogenesis. It is important to remark that both experimental and clinical tumor samples can be analyzed by imBI, as reviewed elsewhere [9] (*see* **Note 2**).

2 Materials

2.1 Cells

The ovarian cancer cell line OC316 was a kind gift of Dr. Silvano Ferrini (IST, Genova, Italy) and can be purchased from the IRCCS AOU San Martino core facility ICLC (http://www.iclc.it).

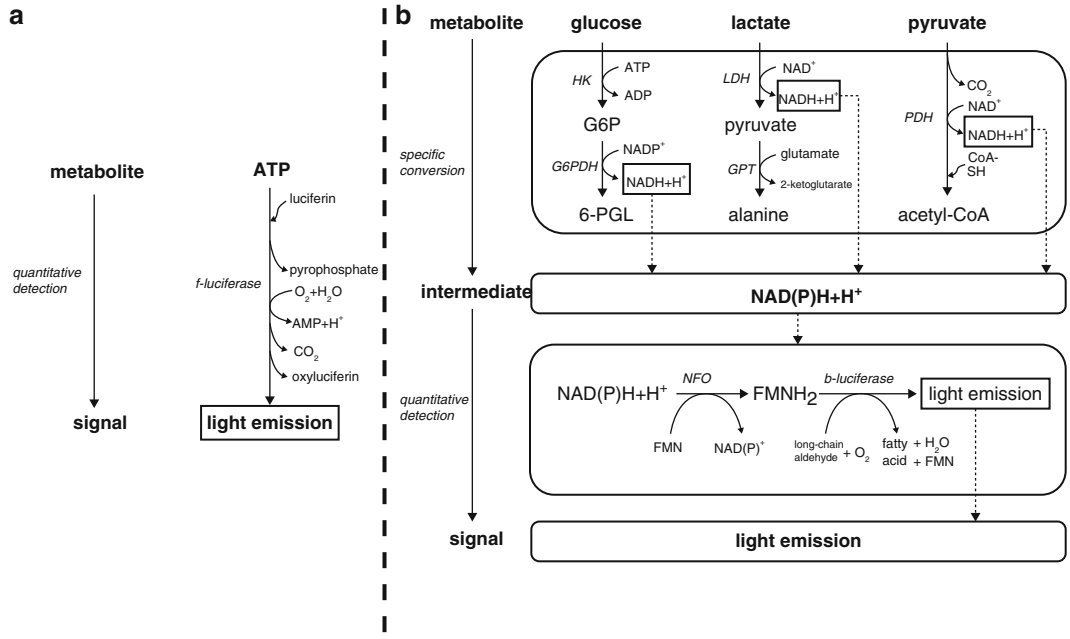

Fig. 1 Schematic of the biochemistry of induced metabolic bioluminescence imaging (imBI): Detection of (**a**) ATP and (**b**) glucose, lactate, pyruvate. (**a**) ATP immediately takes part in the bioluminescence reaction of fireflies (*Photinus pyralis*). (**b**) Glucose, lactate, and pyruvate are enzymatically converted to a common intermediate metabolite, NADH + H^+ or NADPH + H^+. Subsequently, the coenzyme enters the bioluminescence reactions of *Photobacterium fischeri* yielding light emission proportional to the initial metabolite concentration (modified according to [9]). *Abbreviations:* Enzymes: hexokinase (HK), glucose-6-phosphate-dehydrogenase (G6PDH), lactate dehydrogenase (LDH), glucose-pyruvate-transaminase (GPT), pyruvate-dehydrogenase (PDH), NAD(P)H:FMN-oxidoreductase (NFO), bacterial luciferase (b-luciferase), firefly luciferase (f-luciferase). Metabolites: glucose-6-phosphate (G6P), 6-phospho-gluconolactone (6-PGL)

2.2 Mice

Eight-week-old SCID mice were purchased from Charles River (Calco, Italy).

3 Methods

3.1 Generation of Subcutaneous Tumor Xenografts

Procedures involving animals and their care conformed with institutional guidelines that comply with national and international laws and policies (EEC Council Directive 86/609, OJ L 358, 12 December, 1987). For tumor establishment, 8-week-old SCID mice (Charles River) were subcutaneously injected into both flanks with $0.3–0.5 \times 10^6$ tumor cells mixed at 4°C with liquid Matrigel (Becton Dickinson). Tumor volume (mm^3) was calculated as previously reported [8].

Starting from the day of inoculum, the animals were inspected twice weekly and tumors measured by caliper; tumor volume was calculated as $(\text{length} \times \text{width}^2) \times 0.5$. At the end of the experiment,

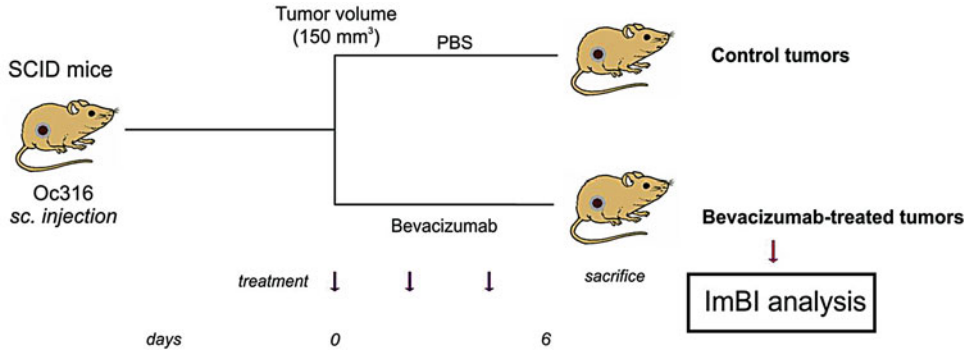

Fig. 2 Schematic of the protocol used to generate subcutaneous tumor xenografts and treatment with the anti-angiogenic drug bevacizumab

the mice were killed by cervical dislocation. The tumors were harvested by dissection, weighted, and snap-frozen in LN2 for imBI analyses (*see* **Note 3**).

3.2 Anti-angiogenic Treatment

In a set of experiments, when the average tumor volume had reached 150 ± 50 mm³, the anti-human VEGF monoclonal antibody (mAb; bevacizumab) was administered intraperitoneally at 100 mg/dose every other day three times, and mice were sacrificed 48 h after the last treatment. Control mice received intraperitoneal injections of PBS (Fig. 2) [8].

3.3 ImBI Analysis

3.3.1 Specific Detection of Tissue Metabolites

1. For processing of the tissue specimens the frozen biopsy is embedded in Tissue Tek® (O.C.T.™ Compound; Sakura Finetek Europe B.V., Alphen aan den Rijn, The Netherlands) on a sample holder of a cryomicrotome (SLEE cryostat, Type MEV; SLEE, Mainz, Germany).
2. Serial sectioning is then performed precisely at a temperature between –20 and –12 °C depending on the tissue composition of the specimen. As indicated in the upper panel of Fig. 3, two parallel channels are driven into each biopsy by a specially designed "micro-fork." Sectioning perpendicular to these channels leads to two holes in each section. These holes make it possible to precisely overlay sequential sections and, thus, to co-localize different parameter values in different adjacent sections.

3.3.2 Localization of Tissue Metabolites

1. The spatial resolution of imBI is generated by a sandwich technique providing a homogeneous contact between enzyme cocktail and tissue section (Fig. 3).
2. An excess volume of enzyme solution is pipetted into a casting mold within a metal slide.
3. A cover glass with a tissue section adhered is laid upside-down onto the enzyme solution within the casting mold. This pro-

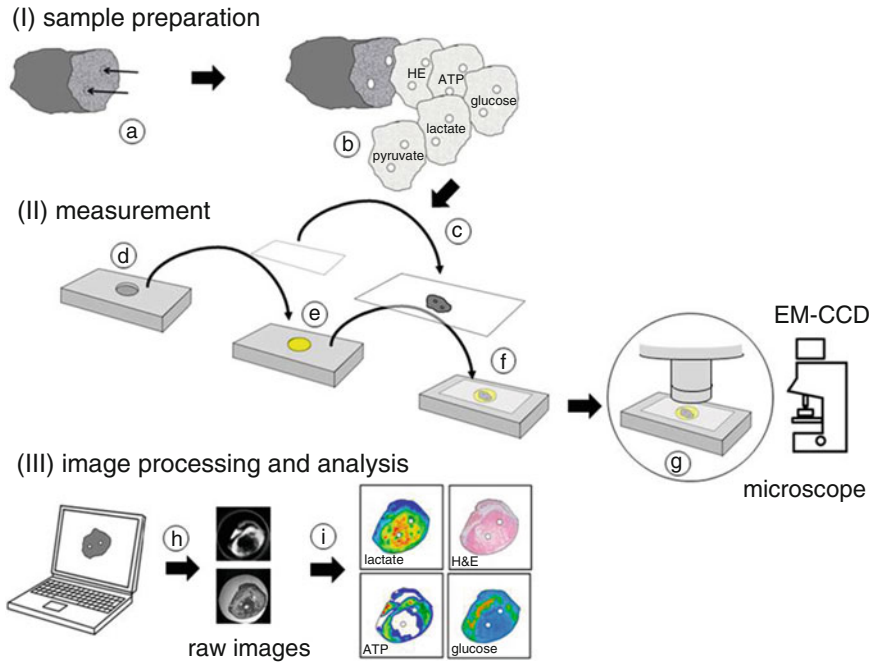

Fig. 3 Schematic of the procedure of induced metabolic bioluminescence imaging (imBI). (*I*) Sample preparation: The frozen tissue sample is precisely punctured by a small fork (**a**). Subsequently, serial cryo-sections are prepared (**b**). Each section is adhered on a cover glass (**c**) and heat-inactivated (not shown). (*II*) A casting mold (**d**) is filled with an appropriate enzyme solution (**e**). Immediately before measurement, a section on a cover glass is immersed into the enzyme solution (**f**). This "sandwich" is inserted into a thermostated chamber mounted on the stage of a microscope (**g**). The light emission is registered by an EM-CCD camera connected to a computer. (*III*) Using an image analysis software (**h**), the raw images are processed, analyzed, calibrated, and finally expressed as color-coded images (**i**). Pinpricks (**a**) within the biopsy provide landmarks for a correct overlay of corresponding images

vides complete contact between tissue and enzyme solution, which has been kept in a liquid state at the measuring temperature. The contact between substrate and enzyme mixture then initiates the bioluminescence reaction.

4. The sandwich is put on the thermostated stage of a microscope (Axiophot, Zeiss, Oberkochen, Germany) within a light-impervious chamber.
5. An ultrasensitive back-illuminated EM-CCD camera (iXonEM+ DU-888; Andor Technology PLC, Belfast, UK) connected to the microscope enables the registration of the low-light bioluminescence intensity with the optics focused on the tissue section plane.
6. The image signal is transferred to a computer for image analysis. By integrating the light emission intensities over a selected time interval, a two-dimensional density profile is obtained representing the two-dimensional metabolite distribution across the tissue section.

3.3.3 Quantification of Tissue Metabolites

1. Using appropriate standards, which are handled in exactly the same way as the tissue of interest, bioluminescence intensities can be transformed into absolute tissue concentrations of the respective metabolite, e.g., in micromoles per gram of tissue (μmol/g) which corresponds approximately to mM in solution.
2. Routine standards are obtained by mixing cryo-embedding medium (Tissue-Tek®) with defined amounts of substrate.
3. The frozen medium is then cryo-sectioned and processed in the same way as the tissue of interest.
4. The calibration allows for the illustration of the two-dimensional substrate distribution in a color-coded manner, as indicated in Fig. 4.

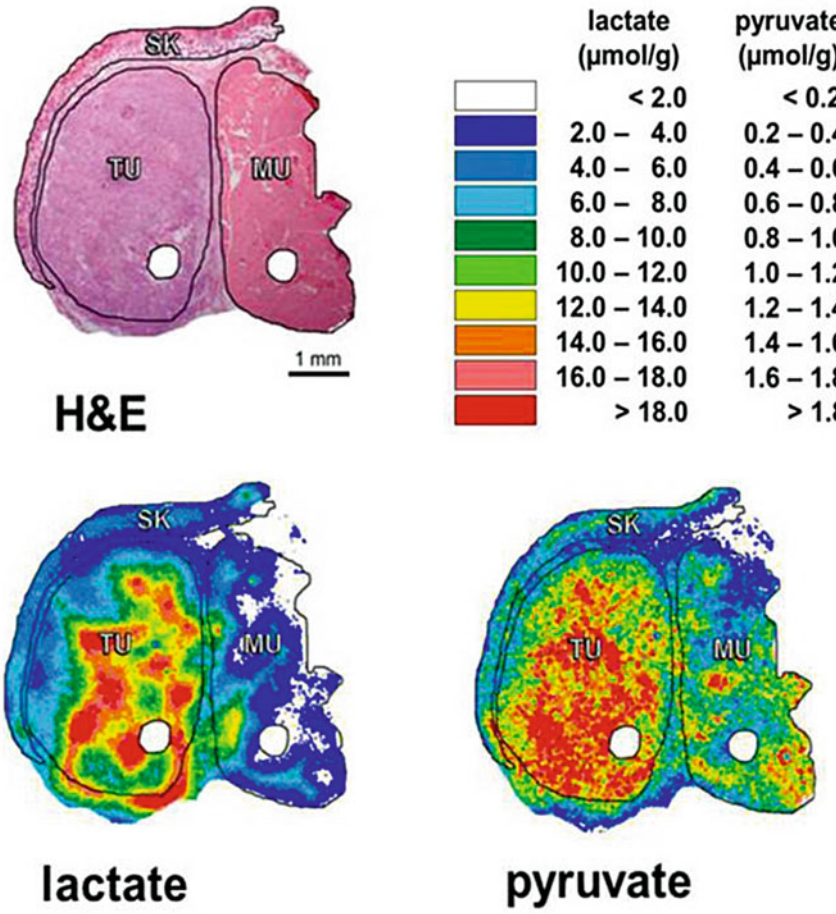

Fig. 4 Induced metabolic bioluminescence imaging (imBI) of lactate and pyruvate in a human head and neck squamous cell carcinoma (HNSCC) xenografted in a nude mouse. Sequential cryo-sections (each showing two punched holes for overlay) were used for hematoxylin and eosin (H&E) staining and imaging of lactate and pyruvate concentrations. For structure-associated evaluation, defined histological areas were delineated: tumor tissue (TU), skeletal muscle (MU), and skin (SK) (modified according to [9])

5. This procedure is applicable to all metabolites specified above.
6. Light intensity is also influenced by the microscopic magnification, since pixel density per unit image area and, hence, light intensity are much lower at a high magnification and vice versa. Other factors with impact on light intensity are the viscosity of the enzyme solution, the measuring temperature, the light integration interval, or the quantum efficiency of the bioluminescence reaction itself. And all these factors are mutually related and not at all independent of each other. In essence, the concert of these factors determines the sensitivity of the technique being on the micromolar level.

3.3.4 Combined Quantification and Localization of Metabolites

1. High sensitivity and high spatial resolution are contradicting demands, but the advantage of imBI is its versatility in adjusting the measuring conditions towards either resolution or sensitivity depending on the requirements of an actual experiment.
2. Spatial resolution is restricted at a low viscosity and high temperature of the enzyme solution and at long light integration interval. Such conditions favor lateral diffusion of metabolites and enzymes resulting in a "smearing out" the gradients in the metabolic profiles.
3. For most measurements in tumor biopsies, experimental settings are chosen in a way that the minimum detectable substrate concentration is around 100 μmol/g with a spatial linear resolution of around 100 μm (*see* **Note 4**).
4. Keeping the former sensitivity of detection, the spatial resolution can be adjusted to 20 μm in imaging metabolic gradients in multicellular spheroids adjusting an appropriate registration temperature and viscosity of the enzyme solution.

3.3.5 Structure-Associated Metabolite Detection and Co-localization

1. Using serial sections, a section can be stained for the histological structure, e.g., with hematoxylin and eosin (H&E), followed by sections stained for the various metabolites.
2. The "two-hole technique" allows for an exact, computer-assisted overlay between the sections. Such an overlay makes it possible to detect the bioluminescence signals in a structure-associated way, i.e., within selected histological areas, such as viable tumor regions, stromal areas, or necrosis. The strategy is exemplified in Fig. 4.
3. Co-localization studies can be extended to virtually all parameters which can be visualized in cryo-sections, e.g., mRNAs detected by in situ hybridization, proteins assessed by immunostaining, or functional parameters, such as blood perfusion imaged by fluorescent stains or hypoxic cells identified by pimonidazole [12].

3.4 Conclusions: Applications of ImBI in the Field of Tumor Angiogenesis

ImBI proved to be an extremely useful technique to investigate modulations in the concentration of metabolites in tumors treated with anti-angiogenic drugs. In tumor xenografts, we observed a dramatic reduction in glucose and ATP levels in the tumor microenvironment following anti-VEGF therapy (Fig. 5) [8]. Such changes, nicely visualized and quantified by imBI, led us to speculate that glucose-addicted tumors could be particularly vulnerable to the effects of VEGF blockade. In line with this prediction, the amount of necrotic area in the highly glycolytic tumors was much larger compared with values found in poorly glycolytic tumors [8], thus connecting a metabolic trait of tumor cells to a histologic pattern of response to VEGF neutralization. Importantly, the hypothesis that highly glycolytic tumors could be highly responsive to antiangiogenic drugs has been recently validated in a clinical trial with the antiangiogenic drug cediranib [13].

4 Notes

1. It is highly recommended that metabolic tissue banks (in liquid nitrogen) should be set up by big clinical centers. We have shown [9] that metabolites can be cryo-preserved for more than 10 years.
2. The speed of cryo-fixation is indeed critical, but it can be done and organized in an appropriate way even in the clinical setting in the operation hall.
3. To prevent loss of ATP, it is critical to remove tumors from the subcutaneous tissue and freeze them in liquid nitrogen within 20 s.
4. In our routine technology, the minimum detectable substrate concentration is around 100 μmol/g of viable tissue. Taking a given thickness of the cryosection used of 10 μm and a section area of 1 cm^2, this corresponds to a minimum detectable absolute amount of substrate (i.e., the substrate content of one cryosection) of around 10 pg. By reducing the section thickness, increasing the enzyme components in the detection cocktails, and optimizing the photon registration technique it is possible to detect minimum substrate concentrations in the nmol/g range.

Funding

This work was supported by grants from AIRC (IG grant 14295), the Deutsche Forschungsgemeinschaft (Mu 576/15-1, 15-2), and the German Federal Ministry of Education and Research ("ISIMEP"; 02NUK016A).

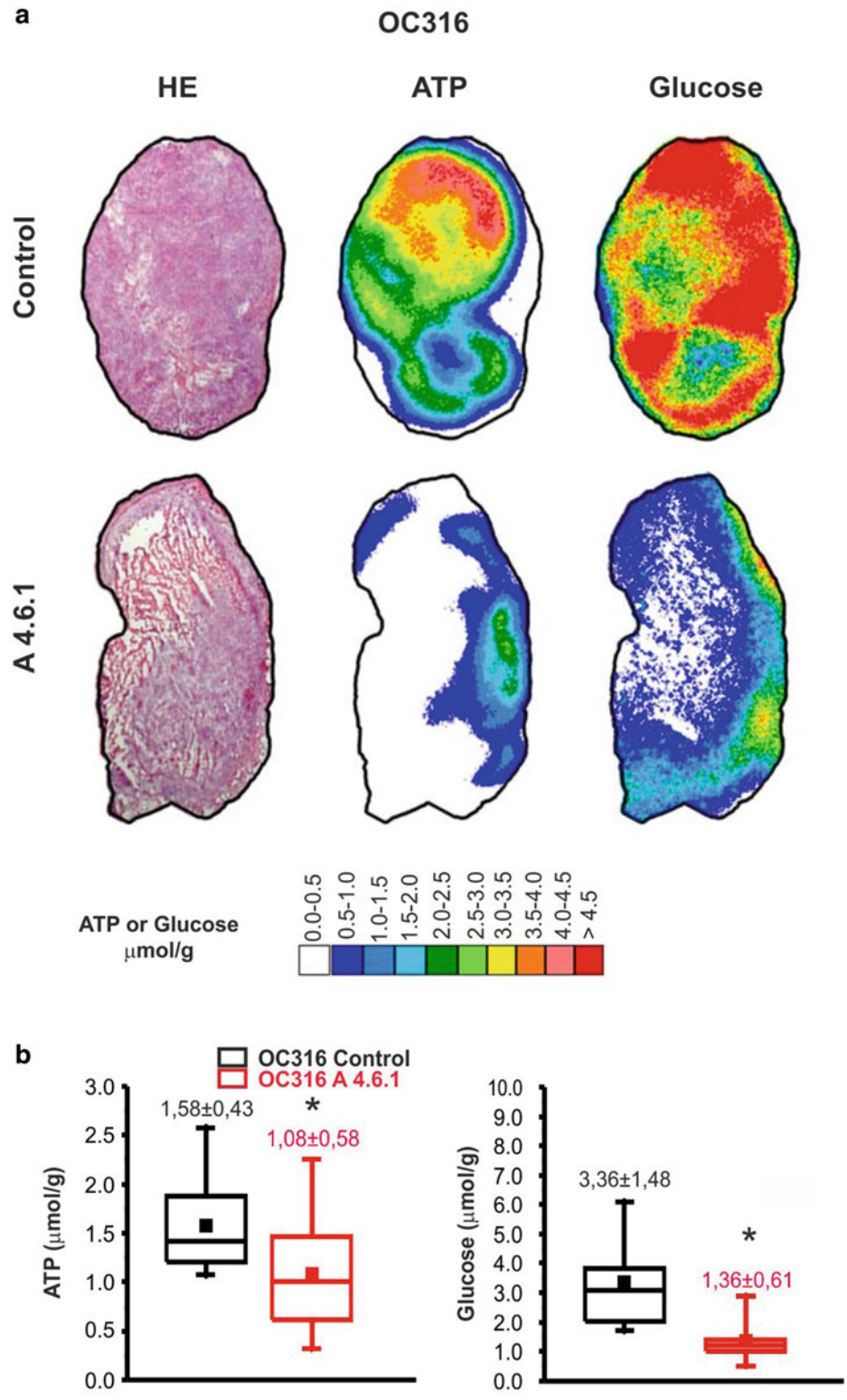

Fig. 5 Metabolic effects of anti-VEGF therapy in tumors measured by bioluminescence imaging. **a**: H&E staining as well as color-coded distributions of ATP and glucose in sequential cryo-sections from representative OC316 tumors treated or not with the anti-VEGF mAb A4.6.1 (100 µg/dose, three doses given every other day). The concentration values were color-coded, with each color corresponding to a defined concentration range in µmol/g. **b**: Metabolite concentrations in OC316 tumors treated or not with A4.6.1. Values were derived exclusively from vital tumor regions. ATP and glucose values were calculated from $n = 12–32$ sections from 4 to 10 different tumors (reproduced from [8])

References

1. Carmeliet P, Jain RK (2011) Principles and mechanisms of vessel normalization for cancer and other angiogenic diseases. Nat Rev Drug Discov 10(6):417–427
2. Grothey A, Galanis E (2009) Targeting angiogenesis: progress with anti-VEGF treatment with large molecules. Nat Rev Clin Oncol 6(9):507–518
3. Heath VL, Bicknell R (2009) Anticancer strategies involving the vasculature. Nat Rev Clin Oncol 6(7):395–404
4. Jayson GC, Hicklin DJ, Ellis LM (2012) Antiangiogenic therapy—evolving view based on clinical trial results. Nat Rev Clin Oncol 9(5):297–303
5. Curtarello M, Zulato E, Nardo G, Valtorta S, Guzzo G, Rossi E, Esposito G, Msaki A, Pasto A, Rasola A et al (2015) VEGF-targeted therapy stably modulates the glycolytic phenotype of tumor cells. Cancer Res 75(1):120–133
6. Bohndiek SE, Kettunen MI, Hu DE, Brindle KM (2012) Hyperpolarized (13)C spectroscopy detects early changes in tumor vasculature and metabolism after VEGF neutralization. Cancer Res 72(4):854–864
7. Keunen O, Johansson M, Oudin A, Sanzey M, Rahim SA, Fack F, Thorsen F, Taxt T, Bartos M, Jirik R et al (2011) Anti-VEGF treatment reduces blood supply and increases tumor cell invasion in glioblastoma. Proc Natl Acad Sci U S A 108(9):3749–3754
8. Nardo G, Favaro E, Curtarello M, Moserle L, Zulato E, Persano L, Rossi E, Esposito G, Crescenzi M, Casanovas O et al (2011) Glycolytic phenotype and AMP kinase modify the pathologic response of tumor xenografts to VEGF neutralization. Cancer Res 71(12):4214–4225
9. Walenta S, Voelxen NF, Sattler UGA, Mueller-Klieser W (2014) Localizing and quantifying metabolites in situ with luminometry: induced metabolic bioluminescence imaging (imBI). In: Hirrlinger J and Waagepetersen HS (eds) Brain energy metabolism. Humana Press (Springer), New York, pp 195–216
10. Walenta S, Mueller-Klieser WF (2004) Lactate: mirror and motor of tumor malignancy. Semin Radiat Oncol 14(3):267–274
11. Walenta S, Schroeder T, Mueller-Klieser W (2004) Lactate in solid malignant tumors: potential basis of a metabolic classification in clinical oncology. Curr Med Chem 11(16):2195–2204
12. Yaromina A, Quennet V, Zips D, Meyer S, Shakirin G, Walenta S, Mueller-Klieser W, Baumann M (2009) Co-localisation of hypoxia and perfusion markers with parameters of glucose metabolism in human squamous cell carcinoma (hSCC) xenografts. Int J Radiat Biol 85(11):972–980
13. Pommier AJ, Farren M, Patel B, Wappett M, Michopoulos F, Smith NR, Kendrew J, Frith J, Huby R, Eberlein C et al (2015) Leptin, BMI, and a metabolic gene expression signature associated with clinical outcome to VEGF inhibition in colorectal cancer. Cell Metab 23(1):77–93